

## Enhanced store-operated calcium entry (SOCE) exacerbates motor neurons apoptosis following spinal cord injury

Jianye Wang<sup>1,\*</sup>, Wenhui Zhao<sup>2,\*</sup>, Xinjun Wang<sup>1</sup>, Haidong Gao<sup>1</sup>, Rongjun Liu<sup>1</sup>, Jixin Shou<sup>1</sup> and Jing Yan<sup>3</sup>

<sup>1</sup> Neurosurgery Department, The Fifth Affiliated Hospital of Zhengzhou University, Zhengzhou, China

<sup>2</sup> Department of Basic Medicine, Jiangsu College of Nursing, Huai'an, China

<sup>3</sup> Physiology Department, Jining Medical University, Jining, China

**Abstract.** Spinal cord injury is pathologically characterized by the loss of motor function caused by neurons apoptosis. Store-operated calcium entry (SOCE) is widely known to dictate the apoptosis of various cell types. To examine SOCE in spinal cord injury and explore the role of SOCE in apoptosis, patients with spinal cord injury (SCI) and SCI mouse models were included. Expression of SOCE components and apoptosis-related proteins were examined by Western blotting. Calcium imaging was used to assess SOCE activity. As a result, we confirmed the enhanced levels of ORAI1 and STIM1 in SCI patients and SCI mouse models. *In vitro* study, tunicamycin impaired the viability of VSC4.1 cells (motoneuron-neuroblastoma hybrid cell line) and increased SOCE activity, the effects of which could be abolished by 2-APB. Furthermore, tunicamycin-reduced BCL-2/BAX ratio was also reversed by 2-APB. Additionally, EdU assay and DCFH-DA staining confirmed the regulatory role of 2-APB in proliferation and ROS production. Of note is the improved hindlimb motor function and alleviated depression by 2-APB administration. Therefore, we conclude that SOCE may contribute to the pathogenesis of SCI by exacerbating the apoptosis of motoneurons.

**Key words:** SOCE — Spinal cord injury — Motor neurons — Apoptosis

**Abbreviations:** EdU, 5-ethynyl-2-deoxyuridine; FCS, fetal calf serum; OD, optical density; PFA, paraformaldehyde; SCI, spinal cord injury; SOCE, store-operated calcium entry.

### Introduction

Spinal cord injury (SCI) is a worldwide debilitating traumatic injury, resulting in a poor quality of life and the heavy burden of the family (Ergun et al. 2002). The primary consequences of SCI are the loss of motor functions, neuropathic pain and depression. However, current medications are not sufficient and associated with unwanted side effects due to the insufficient understanding of the mechanisms. The

pathophysiology of acute SCI includes primary and secondary mechanisms of injury (Oyinbo 2011; Shultz and Zhong 2017). Intracellular calcium ( $\text{Ca}^{2+}$ ) perturbation occurs amid the second mechanism (Lea and Faden 2003; Oyinbo 2011). Given the involvement of  $\text{Ca}^{2+}$  channels in SCI pathology, it logically presents a variety of potential therapeutic targets for the treatment.

$\text{Ca}^{2+}$  channels are involved in a plethora of cellular physiological activities including proliferation, apoptosis and differentiation. Especially,  $\text{Ca}^{2+}$  overload leads to apoptosis, ROS production and reticulum stress (Shumilina et al. 2011; Prakriya and Lewis 2015). The pathogenesis of SCI involves various types of  $\text{Ca}^{2+}$  channels, including L/N-type  $\text{Ca}^{2+}$  channels (Agrawal et al. 2000; Nehrt et al. 2007), inositol (1,4,5)-triphosphate ( $\text{IP}_3$ ) and ryanodine receptors (Thorell et al. 2002). Store-operated calcium

**Electronic supplementary material.** The online version of this article (doi: 10.4149/gpb\_2020040) contains Supplementary Material.

\* These authors participated equally to this study.

**Correspondence to:** Jing Yan, Physiology Department, Jining Medical University, Jining, China  
E-mail: yanjing102@mail.jnmc.edu.cn

channel (SOCC), also termed as  $\text{Ca}^{2+}$ -released activated  $\text{Ca}^{2+}$  channel (CRAC), is a major pathway for  $\text{Ca}^{2+}$  influx in non-excitabile cells and plays a pivotal role in the physiological functions of various cell types. Briefly, release from intracellular stores and subsequent intracellular  $\text{Ca}^{2+}$  stores depletion induce the activation of store-operated  $\text{Ca}^{2+}$  entry (SOCE). SOCE is accomplished by the pore-forming  $\text{Ca}^{2+}$  channel subunits ORAI1, ORAI2, and ORAI3 as well as their regulators STIM1 and STIM2 (Mignen et al. 2008). It has been well documented that SOCE regulates various cellular functions including migration, apoptosis, proliferation, and interleukins release (Yan et al. 2016a, 2016b). Moreover, accumulated evidence indicate that SOCE activity contributes to normal neuronal activity (Sukkar et al. 2018; Maciag et al. 2019; Majewski et al. 2020). Of note is the enhanced  $\text{Ca}^{2+}$  release from intracellular  $\text{Ca}^{2+}$  stores after trauma, contributing to the loss of functions in white matter of brain and spinal cord (Thorell et al. 2002). However, the role of SOCE in the pathogenesis of SCI remains elusive.

In the present study, we confirmed the enhanced expression of ORAI1 and STIM1 as well as SOCE activity *in vivo* and *in vitro* studies, explored the role for SOCE in motor neurons apoptosis, provided a potential alternative for SCI treatment.

## Materials and Methods

### Patient samples

A total of random 28 patients with spinal cord injury at the Fifth Affiliated Hospital of Zhengzhou University were chosen for this study. All patients gave written informed consent. Written informed consent was obtained from all patients who participated in the study, and the study was approved by Jining medical university ethics review board. Blood Samples were collected from patients, and then serum was separated after centrifugation at  $2800 \times g$  for 8 min and stored at  $-80^{\circ}\text{C}$ .

### Animal model of spinal cord injury

C57BL/6J were purchased from the Animal Center of the Chinese Academy of Sciences of Shanghai, China. Procedures with experimental animals were approved by the Animal Care and Use Committee of Jining medical university. Adult male mice (8–10 weeks of age) weighing approximately 20 g were anesthetized. Along the midline of the dorsum to expose the vertebral column, transection of the spinal cord at T4 level was performed in SCI models ( $n = 21$ ). Sham group underwent the same surgical procedure but not transected ( $n = 10$ ).

### Cell culture

VSC4.1 cells were maintained on culture dishes (Nest technology) coated with poly-L-ornithine (PLO) (Sigma) in DMEM:F12 (1:1) containing Glutamax supplemented with 2% FBS, 1% N1 (Sigma) and 1% NEAA (referred to as VSC4.1 complete medium).

### Cell viability assay

VSC4.1 cells were grown in DMEM medium supplemented with 10% FCS (fetal calf serum) and 1% penicillin/streptomycin. The cells were incubated with 5%  $\text{CO}_2$  at  $37^{\circ}\text{C}$  in a humidified incubator. The medium was replaced every 24 hours. Cells were grown to about 80% confluence prior to tunicamycin (TM) treatment.

To explore the effects of tunicamycin-induced apoptosis, cells were treated with tunicamycin at different concentrations (100 nM, 1  $\mu\text{M}$ , 10  $\mu\text{M}$ ). Each group of cells was seeded in 96-well microtiter plates and incubated for 12 h. At different points, 20  $\mu\text{l}$  of MTT was added to each well followed by 4-h incubation. The OD (optical density) was measured at 492 nm after 4 h DMSO incubation. The proliferation inhibition rate was calculated as:  $(1 - \text{OD of the experimental group} / \text{OD of the control group}) \times 100\%$ .

### Western blot

Cells were washed twice in ice-cold PBS. RIPA lysis buffer (Cell Signaling, United states) containing phosphatase and protease inhibitor cocktail tablet (Thermo Fisher Scientific, United States) was added to the washed cells. The samples were incubated on ice for 30 min and then centrifuged at 14,000 rpm and  $4^{\circ}\text{C}$  for 20 min. The supernatant was removed and used for Western blotting. Total protein (40  $\mu\text{g}$ ) was separated by SDS-PAGE, transferred to PVDF membranes and blocked in 5% non-fat milk/Tris-buffered saline/Tween-20 (TBST, PH 7.4) at room temperature for 30 min. Membranes were incubated overnight at  $4^{\circ}\text{C}$  with BCL-2 and BAX (Abcam, 1:1000), ORAI1 (Abcam, 1:200), STIM1 and GAPDH antibodies (Sigma, United States, 1:1000). After incubation with horseradish peroxidase-conjugated anti-rabbit secondary antibody (Sigma, 1:1000) for 2 h at room temperature, the bands were visualized with enhanced chemiluminescence reagents (Sigma). Densitometric analysis was performed using Quantity One software, all original blots were put in Supplementary Material (see Figure S1).

### Immunofluorescent assay

Cells were washed twice in ice-cold PBS and incubated with EdU (5-ethynyl-2-deoxyuridine) (50  $\mu\text{M}$ ) for 2 h. After PBS

washing two times, cells were fixed in 4% PFA (paraformaldehyde) for 30 min and then treated with glycine 2 mg/ml for 5 min. 0.5% TritonX-100 was administered after washing, Apollo and Dapi staining were performed according to the instructions (Click-iT EdU kit, Thermofisher).

DCFH-DA (6-carboxy-2',7'-dichlorodihydrofluorescein diacetate) staining was performed according to the instructions (Thermofisher). Briefly, cells were incubated with DCFH-DA dye solution for 60 min and changed into the growth medium. After Dapi staining, cells were visualized.

#### qRT-PCR

Total RNA was extracted with Takara RNA extraction kit. Reverse transcription of total RNA was performed using Transcriptor High Fidelity cDNA Synthesis Kit (TAKARA). Real-time polymerase chain reaction (RT-PCR) of the respective genes were set up in a total volume of 20  $\mu$ l using 40 ng of cDNA, 500 nM forward and reverse primer and 2 $\times$  GoTaq<sup>®</sup> qPCR Master Mix (Promega) according to the manufacturer's protocol. Cycling conditions were as follows: initial denaturation at 95°C for 2 min, followed by 40 cycles of 95°C for 15 s, 58°C for 15 s and 68°C for 20 s. For amplification the following primers were used (5'>3' orientation): The following primers were used: for *tbp*: forward (5'-3'): ACTCTGCCACACCAGCC, reverse (5'-3'): GGTCAAGTTTACAGCCAAGATTCA; for *orai1*: forward (5'-3'): CGTCCACAACCTCAACTCC, reverse (5'-3'): AACTGTCCGGTCCGTCTTAT; for *stim1*: forward (5'-3'): CGTCCGCAACATCCACAAG, reverse (5'-3'): CCATAGGTCCTCCACGCT.

Specificity of PCR products was confirmed by analysis of a melting curve. Real-time PCR amplifications were performed on a CFX96 Real-Time System (Bio-Rad) and all experiments were done in duplicate. GAPDH was amplified to standardize the amount of sample RNA. Relative quantification of gene expression was achieved using the  $\Delta$ CT method as described.

#### Ca<sup>2+</sup> measurements

Cells were loaded with Fura-2/AM (2  $\mu$ M, Invitrogen) for 15 min at 37°C (Yan et al. 2018). Cells were excited alternatively at 340 nm and 380 nm through an objective (Fluor 40 $\times$ 1.30 oil) built in an inverted phase-contrast microscope (Axiovert 100, Zeiss). Emitted fluorescence intensity was recorded at 505 nm. Data were acquired using specialized computer software (Metafluor, USA). Cytosolic Ca<sup>2+</sup> activity was estimated from the 340 nm/380 nm ratio. SOCE was determined by extracellular Ca<sup>2+</sup> removal and subsequent Ca<sup>2+</sup> re-addition in the presence of thapsigargin (1  $\mu$ M, Invitrogen). For quantification of Ca<sup>2+</sup> entry, the slope (delta ratio/s) and peak (delta ratio) were calculated fol-

lowing re-addition of Ca<sup>2+</sup>. SOCE activity was suppressed by 2-APB, whereas not affected by nifedipine (L-type Ca<sup>2+</sup> channel), confirming the validity of this methodology (see Supplementary Material, Figure S2).

#### Basso mouse scale (BMS)

BMS was performed to measure the recovery of hindlimb motor function in six mice on 1, 3, 14, 21 days following SCI surgery.

#### Sucrose preference test

Sucrose preference percentage (%) = (sucrose solution consumption)/(sucrose solution consumption + water consumption)  $\times$  100%. All mice were feed with 200 ml of water and 2% sucrose solution. The consumed water and sucrose solution were recorded after 12 h.

#### Statistics

Data are provided as means  $\pm$  SEM, *n* represents the number of independent experiments. All data were tested for significance using one-way ANOVA followed by *post hoc* Bonferroni test applied when multiple comparisons between different groups were made. Only results with *p* < 0.05 were considered statistically significant.

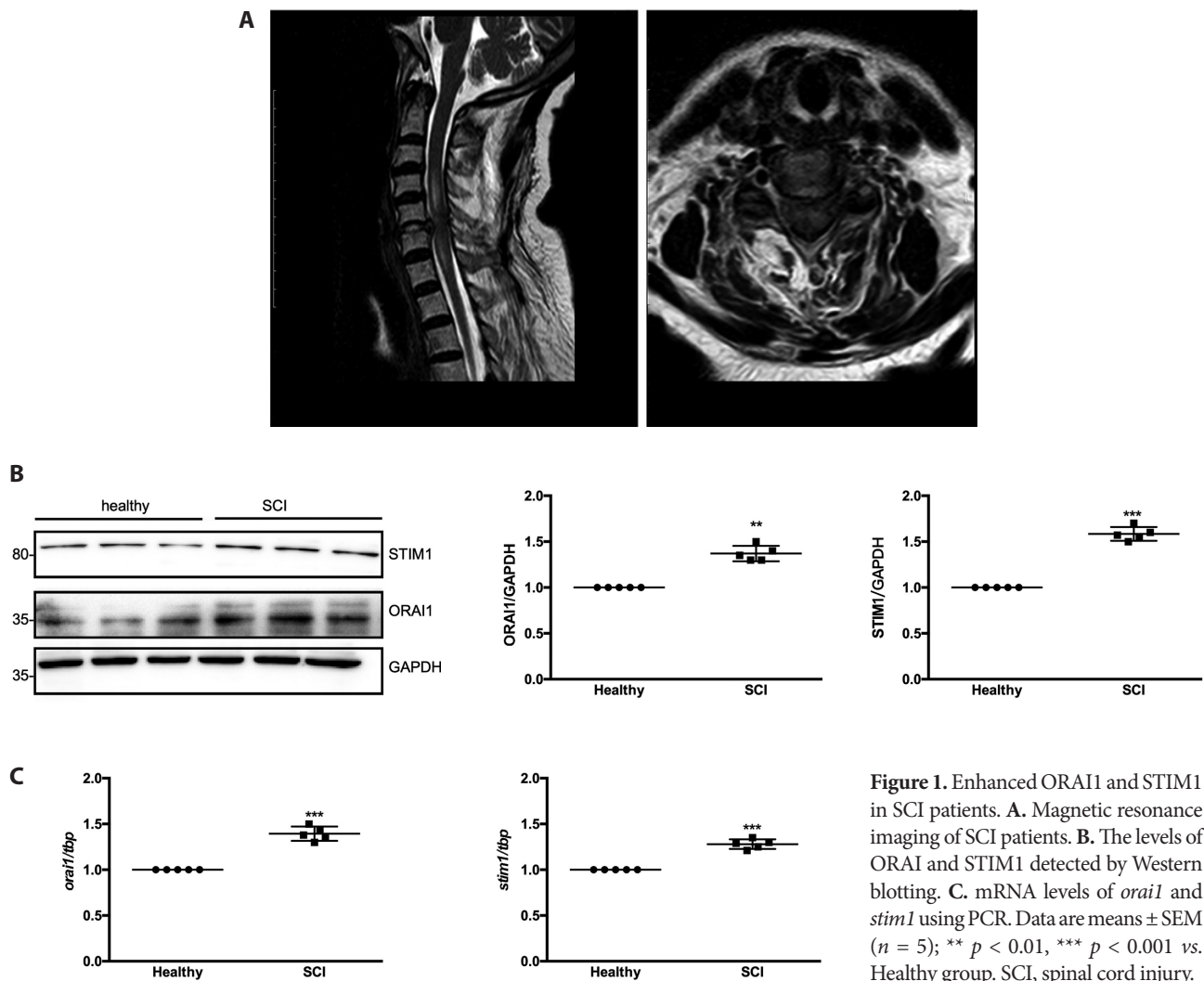
## Results

#### Increased ORAI1 and STIM1 in patients with SCI

We first identified the SCI patients by magnetic resonance imaging (Fig. 1A) and assessed the levels of ORAI1 and STIM1 in the blood from SCI patients. As illustrated in Figure 1B, Western blotting demonstrated that ORAI1 and STIM1 levels in SCI group were significantly higher than that in healthy subjects. Moreover, RT-PCR results confirmed the elevated mRNA levels of *orai1* and *stim1* in SCI group (Fig. 1C), suggesting the involvement of SOCE in human SCI.

#### Increased ORAI1 and STIM1 in SCI mouse models and in vitro study

To assess whether the findings above in SCI patients are consistent with SCI mouse models, Western blotting and RT-PCR were performed. As shown in Figure 2A, Western blotting showed that both ORAI1 and STIM1 protein abundance were elevated in SCI group compared with sham group, which is further supported by RT-PCR results (Fig. 2B).



Given that tunicamycin (Smith et al. 2012) could be used to mimic the pathological condition of SCI by facilitating the apoptosis of neurons (Akiyama et al. 2016; Nami et al. 2016), tunicamycin was included to establish the cellular model of SCI. MTT assay showed that tunicamycin induced the apoptosis of VSC4.1 neurons in a dose-dependent and time-dependent manner (Fig. 2C), and 1  $\mu$ M tunicamycin was chosen. We then treated VSC4.1 neurons with tunicamycin (1  $\mu$ M) to ascertain the levels of ORAI1 and STIM1 *in vitro*. Expectedly, both ORAI1 and STIM1 protein and mRNA levels were significantly enhanced after tunicamycin treatment (Fig. 2D and E), confirming the role for SOCE in SCI pathology.

#### Tunicamycin increased SOCC in VSC4.1 neurons

Fura-2  $\text{Ca}^{2+}$  imaging was performed to examine SOCE activity. Thapsigargin, a sarco-endoplasmic reticulum  $\text{Ca}^{2+}$

ATPase inhibitor, blocks  $\text{Ca}^{2+}$  refilling into endoplasmic reticulum (ER). Herein, thapsigargin was used to empty  $\text{Ca}^{2+}$  store and thus initiate SOCE. As illustrated in Figure 3, both  $\text{Ca}^{2+}$  release from  $\text{Ca}^{2+}$  store and  $\text{Ca}^{2+}$  entry were increased after tunicamycin treatment. Peak and slope represents the amplitude and the velocity, respectively. 2-Aminoethyl diphenylborinate (2-APB) is a cell-permeable inhibitor of  $\text{IP}_3\text{R}$  and also inhibits SOCE at 100  $\mu$ M (Figure S2). 2-APB administration significantly abolished tunicamycin-induced SOCE, indicating the involvement of SOCE in the progression of SCI.

#### 2-APB alleviated tunicamycin-induced neurons apoptosis

As demonstrated by Figure 4A, MTT assay showed that tunicamycin-induced apoptosis was markedly blunted by 2-APB. Moreover, B-cell lymphoma-2 (BCL-2) and BCL-2-associated X protein (BAX) are apoptosis-related proteins,

and our Western blotting results found that tunicamycin administration increased BAX expression and decreased BCL-2 level (Fig. 4B), an effect of which could be abolished by 2-APB. Additionally, EdU assay showed that the reduced proliferation capacity by tunicamycin was reversed after 2-APB treatment for 2 hours (Fig. 4C), which confirms that tunicamycin facilitated apoptosis by up-regulating SOCE activity.

Ca<sup>2+</sup> overload-induced apoptosis associates with mitochondrial activities; we utilized DCFH-DA assay to examine reactive oxygen species (ROS). As illustrated in Figure 4D, tunicamycin dramatically exacerbated mitochondrial stress, an effect of which was also inhibited by 2-APB. Furthermore, BMS score and sucrose preference tests were conducted to detect the hindlimb motor function and the depressive status,

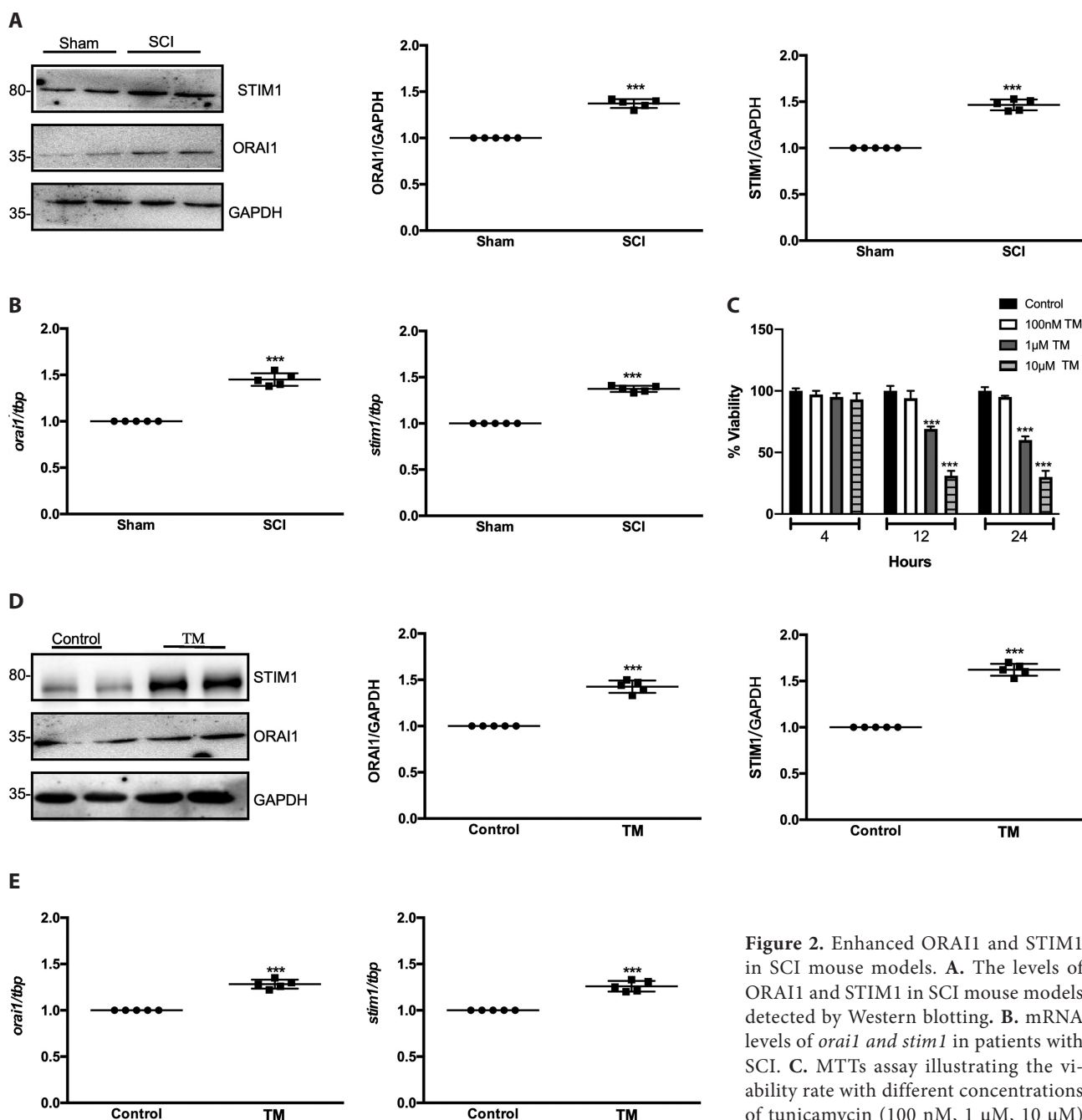


**Figure 2.** Enhanced ORAI1 and STIM1 in SCI mouse models. **A.** The levels of ORAI1 and STIM1 in SCI mouse models detected by Western blotting. **B.** mRNA levels of *orai1* and *stim1* in patients with SCI. **C.** MTTs assay illustrating the viability rate with different concentrations of tunicamycin (100 nM, 1 µM, 10 µM) at different time points (4, 12, 24 h). The

levels of ORAI1 and STIM1 (**D**) and mRNA levels of *orai1* and *stim1* (**E**) in VSC4.1 neurons treated with tunicamycin for 12 h. \*\*\*  $p < 0.001$  vs. Sham, Control group. SCI, spinal cord injury; TM, tunicamycin.

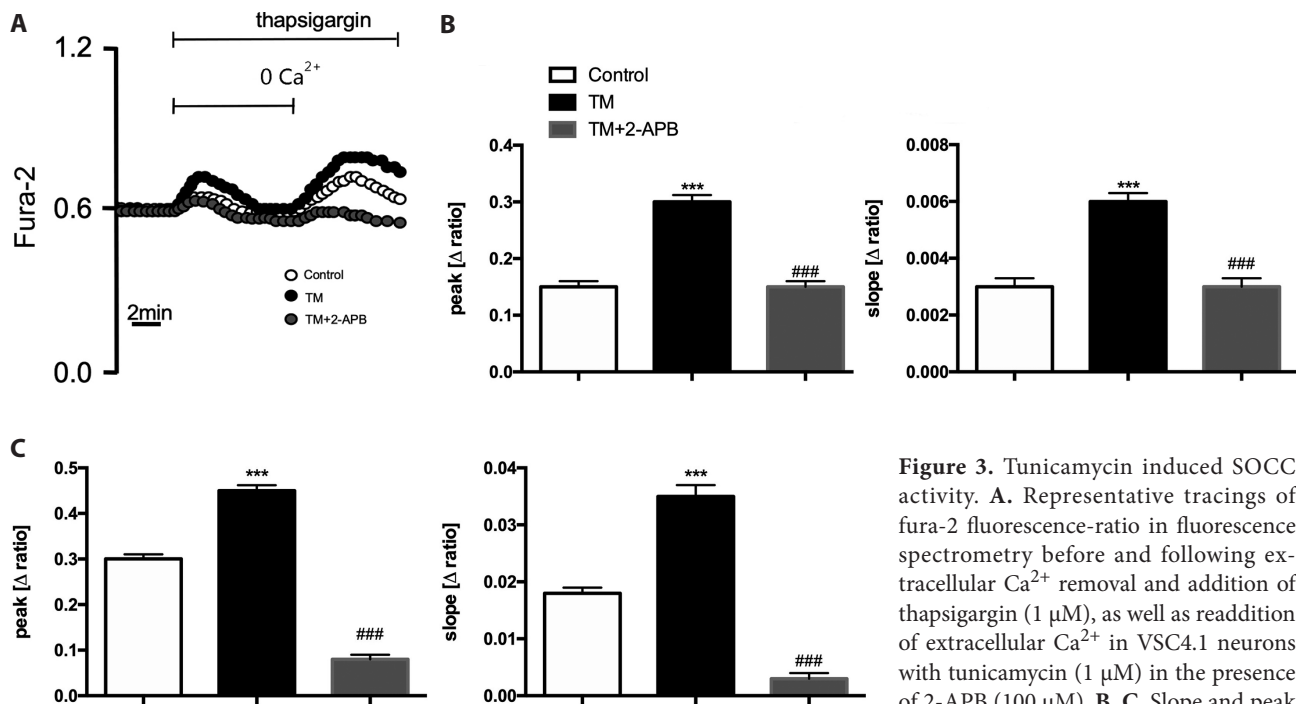


**Figure 3.** Tunicamycin induced SOCC activity. **A.** Representative tracings of fura-2 fluorescence ratio in fluorescence spectrometry before and following extracellular  $\text{Ca}^{2+}$  removal and addition of thapsigargin ( $1 \mu\text{M}$ ), as well as readdition of extracellular  $\text{Ca}^{2+}$  in VSC4.1 neurons with tunicamycin ( $1 \mu\text{M}$ ) in the presence of 2-APB ( $100 \mu\text{M}$ ). **B, C.** Slope and peak increase of fura-2-fluorescence-ratio fol-

lowing addition of thapsigargin ( $1 \mu\text{M}$ ) following extracellular  $\text{Ca}^{2+}$  removal (B) and re-addition of extracellular  $\text{Ca}^{2+}$  reflecting SOCE (C) in VSC4.1 neurons with tunicamycin ( $1 \mu\text{M}$ ) in the presence of 2-APB ( $100 \mu\text{M}$ ) ( $n = 39\text{--}43$  cells). \*\*\*  $p < 0.001$  vs. Control group, ###  $p < 0.001$  vs. TM group. TM, tunicamycin.

respectively. Additionally, 2-APB administration improved the function of the hindlimb (Fig. 4E) and markedly alleviated SCI-caused depression (Fig. 4F) of mouse models.

## Discussion

The pathogenesis of SCI is associated with the perturbations in cellular  $\text{Ca}^{2+}$  homeostasis and ensuing neuronal excitotoxicity (Matute 2010; Del Rivero and Bethea 2016; He et al. 2017). Various types of calcium channels thus play a critical role in the progression of SCI (Agrawal et al. 2000; Thorell et al. 2002; Nehrt et al. 2007). Noteworthy is that SOCE activity is involved in many diseases, including cancer (Yan et al. 2016a), inflammation (Yan et al. 2019) and traumatic injury (Thorell et al. 2002). However, whether SOCE contributes to SCI is unknown.

SOCE components are broadly expressed in human tissues, including brain (Berna-Erro et al. 2009; Klejman et al. 2009; Soboloff et al. 2012; Hou et al. 2015), and SOCE has been implicated in neuronal calcium signaling even before the establishment of its components (Soboloff et al. 2012).

Agrawal and colleagues found that inhibition of SOCE confers significant improvement in compound action potential amplitude after injury (Thorell et al. 2002). Our results

showed that 2-APB markedly alleviated the depression and improved the motor function of SCI mouse models, indicating that SOCE might be a potential therapeutic alternative for SCI.

Proper intracellular  $\text{Ca}^{2+}$  concentration maintains the normal cellular physiological processes, including survival and apoptosis. We found that 2-APB significantly suppressed tunicamycin-induced apoptosis of motor neurons. Given the well-documented inhibitory role of 2-APB in SOCE, we propose that SOCE induces the apoptosis of motor neurons by causing calcium overload. Each SOCE component has its unique virtue of regulating apoptosis (Tanwar and Motiani 2018). As the major components of SOCE, ORAI1 and STIM1 associate with SOCE in neurons (Klejman et al. 2009) and are responsible for mitochondrial calcium overload. Importantly, either *orai1* or *stim1* deficiency renders cells protection from mitochondrial-mediated cell death progression (Tanwar and Motiani 2018). Hou et al. (2015) reported that traumatic injury-induced neuronal cell death is driven by the up-regulation of STIM1. Consistently, herein we confirmed that both ORAI1 and STIM1 were increased in SCI patients and SCI mouse models as well as *in vitro* models, supporting the critical role for ORAI1 and STIM1 in neurons apoptosis. Altogether, ORAI1 and STIM1 appear to be potential therapeutic alternatives for SCI treatment.

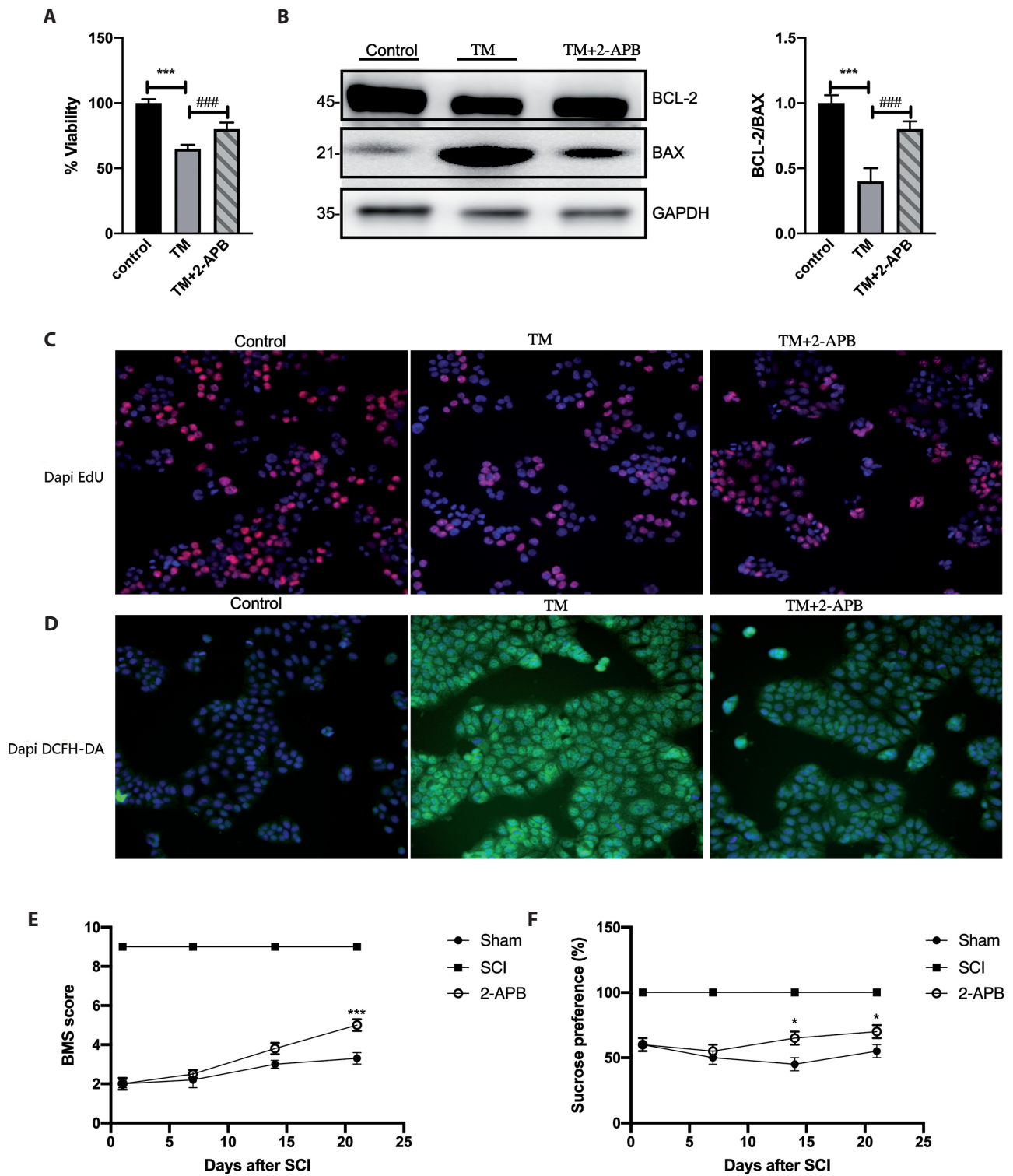


**Figure 4.** Tunicamycin-induced apoptosis of VSC4.1 motoneurons was SOCE sensitive. **A.** The viability rate illustrated by MTT assay. **B.** The protein levels of BAX and BCL-2 in VSC4.1 neurons detected by Western blotting. **C.** EdU assay showing the proliferation of VSC4.1 neurons. **D.** DCFH-DA staining showing the mitochondrial stress of VSC4.1 neurons. The neurons (in B, C, D) were treated with tunicamycin (1  $\mu$ M) in the presence of 2-APB (100  $\mu$ M). The BMC score (**E**) and the sucrose preference score (**F**) of SCI mouse models administered intraperitoneally with 0.5 mg/kg 2-APB. \*  $p < 0.05$ , \*\*\*  $p < 0.001$  vs. Control or Sham group; ###  $p < 0.001$  vs. TM group. SCI, spinal cord injury; TM, tunicamycin.

In comparison to ORAI1 and STIM1, ORAI2 and STIM2 support a moderate steady-state SOCE. STIM2 is involved in hypoxic neuronal cell death (Berna-Erro et al. 2009) and glutamate-induced excitotoxicity (Sodero et al. 2012) in acute neuronal injury and neurodegenerative diseases. STIM2 deficiency leads to loss of mushroom spines and is responsible for memory loss (Sun et al. 2014). Furthermore, Rao et al. (2015) found that *stim2* deficiency alleviated mitochondrial  $\text{Ca}^{2+}$  levels and improved neuronal cell survival after traumatic brain injury. Likewise, *stim2* deficiency contributes to the apoptosis resistance in neurons and colon cancer cells (Berna-Erro et al. 2009, Sobradillo et al. 2014), supporting the involvement of STIM2 in the cellular apoptotic pathways. Of interest is that ORAI3 facilitates 2-APB-induced endoplasmic reticulum calcium leak and limits the calcium overloading of the ER store (Leon-Aparicio et al. 2017), which suggests a possible apoptosis resistance virtue of ORAI3. Additionally, 2-APB also inhibits TRPCs (transient receptor potential channels) (Fels et al. 2018), so extensive exploration is needed to clarify the rationales that could illustrate the role of TRPCs in apoptosis.

Taken together, our findings demonstrated that ORAI1 and STIM1-mediated SOCE contributes to the apoptosis in motoneurons through elevating ROS production and thus exacerbates the progression of SCI. Therefore, the present study provides a new therapeutic alternative for SCI.

**Conflict of interest.** All authors disclose that they have not any potential conflict of interest (e.g., consultancies, stock ownership, equity interests, patent-licensing arrangements, lack of access to data, or lack of control of the decision to publish).

**Acknowledgement.** This work was supported by National Natural Science Fund of China (Grant 31801172) and the Young Talent Project (2019HYTP031) of Henan Province.

## References

- Agrawal SK, Nashmi R, Fehlings MG (2000): Role of L- and N-type calcium channels in the pathophysiology of traumatic spinal cord white matter injury. *Neuroscience* **99**, 179-188  
[https://doi.org/10.1016/S0306-4522\(00\)00165-2](https://doi.org/10.1016/S0306-4522(00)00165-2)
- Akiyama T, Oishi K, Wullaert A (2016): Bifidobacteria prevent tunicamycin-induced endoplasmic reticulum stress and subsequent barrier disruption in human intestinal epithelial Caco-2 monolayers. *PLoS One* **11**, e0162448  
<https://doi.org/10.1371/journal.pone.0162448>
- Berna-Erro A, Braun A, Kraft R, Kleinschnitz C, Schuhmann MK, Stegner D, Wulsch T, Eilers J, Meuth SG, Stoll G, Nieswandt B (2009): STIM2 regulates capacitive  $\text{Ca}^{2+}$  entry in neurons and plays a key role in hypoxic neuronal cell death. *Sci. Signal.* **2**, ra67  
<https://doi.org/10.1126/scisignal.2000522>
- Del Rivero T, Bethea JR (2016): The effects of spinal cord injury on bone loss and dysregulation of the calcium/parathyroid hormone loop in mice. *Osteoporos Sarcopenia* **2**, 164-169  
<https://doi.org/10.1016/j.afos.2016.06.003>
- Ergun R, Akdemir G, Sen S, Tasci A, Ergunor F (2002): Neuroprotective effects of propofol following global cerebral ischemia in rats. *Neurosurg. Rev.* **25**, 95-98  
<https://doi.org/10.1007/s101430100171>
- Fels B, Bulk E, Pethő Z, Schwab A (2018): The role of TRP channels in the metastatic cascade. *Pharmaceuticals (Basel)* **11**, 48  
<https://doi.org/10.3390/ph11020048>
- He W, Sun JF, Jiang RY, Zhang ZJ, Chen Q, Huang YH (2017): Effect of calcium-sensing receptor on the apoptosis of rat spinal cord neurons in anoxia/reoxygenation injury and its significance. *Zhongguo Yi Xue Ke Xue Yuan Xue Bao* **39**, 623-628 (in Chinese)
- Hou PF, Liu ZH, Li N, Cheng WJ, Guo SW (2015): Knockdown of STIM1 improves neuronal survival after traumatic neuronal injury through regulating mGluR1-dependent  $\text{Ca}^{2+}$  signaling in mouse cortical neurons. *Cell. Mol. Neurobiol.* **35**, 283-292  
<https://doi.org/10.1007/s10571-014-0123-0>
- Klejman ME, Gruszczynska-Biegala J, Skibinska-Kijek A, Wisniewska MB, Misztal K, Blazejczyk M, Bojarski L, Kuznicki J (2009): Expression of STIM1 in brain and puncta-like colocalization of STIM1 and ORAI1 upon depletion of  $\text{Ca}^{2+}$  store in neurons. *Neurochem. Int.* **54**, 49-55  
<https://doi.org/10.1016/j.neuint.2008.10.005>
- Lea PMT, Faden AI (2003): Modulation of metabotropic glutamate receptors as potential treatment for acute and chronic neurodegenerative disorders. *Drug News Perspect.* **16**, 513-522  
<https://doi.org/10.1358/dnp.2003.16.8.829350>
- Leon-Aparicio D, Pacheco J, Chavez-Reyes J, Galindo JM, Valdes J, Vaca L, Guerrero-Hernandez A (2017): Orai3 channel is the 2-APB-induced endoplasmic reticulum calcium leak. *Cell Calcium* **65**, 91-101  
<https://doi.org/10.1016/j.ceca.2017.01.012>
- Maciag F, Majewski L, Boguszewski PM, Gupta RK, Wasilewska I, Wojtas B, Kuznicki J (2019): Behavioral and electrophysiological changes in female mice overexpressing ORAI1 in neurons. *Biochim. Biophys. Acta Mol. Cell Res.* **1866**, 1137-1150  
<https://doi.org/10.1016/j.bbamcr.2019.01.007>
- Majewski L, Maciag F, Boguszewski PM, Kuznicki J (2020): Transgenic mice overexpressing human STIM2 and ORAI1 in neurons exhibit changes in behavior and calcium homeostasis but show no signs of neurodegeneration. *Int. J. Mol. Sci.* **21**, 842  
<https://doi.org/10.3390/ijms21030842>
- Matute C (2010): Calcium dyshomeostasis in white matter pathology. *Cell Calcium* **47**, 150-157  
<https://doi.org/10.1016/j.ceca.2009.12.004>
- Mignen O, Thompson JL, Shuttleworth TJ (2008): Orai1 subunit stoichiometry of the mammalian CRAC channel pore. *J. Physiol.* **586**, 419-425  
<https://doi.org/10.1113/jphysiol.2007.147249>
- Nami B, Donmez H, Kocak N (2016): Tunicamycin-induced endoplasmic reticulum stress reduces in vitro subpopulation and invasion of CD44+/CD24- phenotype breast cancer stem cells. *Exp. Toxicol. Pathol.* **68**, 419-426  
<https://doi.org/10.1016/j.etp.2016.06.004>

- Nehrt A, Rodgers R, Shapiro S, Borgens R, Shi R (2007): The critical role of voltage-dependent calcium channel in axonal repair following mechanical trauma. *Neuroscience* **146**, 1504-1512  
<https://doi.org/10.1016/j.neuroscience.2007.02.015>
- Oyinbo CA (2011): Secondary injury mechanisms in traumatic spinal cord injury: a nugget of this multiply cascade. *Acta Neurobiol. Exp. (Wars)* **71**, 281-299
- Prakriya M, Lewis RS (2015): Store-operated calcium channels. *Physiol. Rev.* **95**, 1383-1436  
<https://doi.org/10.1152/physrev.00020.2014>
- Rao W, Zhang L, Peng C, Hui H, Wang K, Su N, Wang L, Dai SH, Yang YF, Chen T, et al (2015): Downregulation of STIM2 improves neuronal survival after traumatic brain injury by alleviating calcium overload and mitochondrial dysfunction. *Biochim. Biophys. Acta* **1852**, 2402-2413  
<https://doi.org/10.1016/j.bbadis.2015.08.014>
- Shultz RB, Zhong Y (2017): Minocycline targets multiple secondary injury mechanisms in traumatic spinal cord injury. *Neural Regen. Res.* **12**, 702-713  
<https://doi.org/10.4103/1673-5374.206633>
- Shumilina E, Huber SM, Lang F (2011): Ca<sup>2+</sup> signaling in the regulation of dendritic cell functions. *Am. J. Physiol. Cell Physiol.* **300**, C1205-1214  
<https://doi.org/10.1152/ajpcell.00039.2011>
- Smith MC, Williamson J, Yaster M, Boyd GJ, Heitmiller ES (2012): Off-label use of medications in children undergoing sedation and anesthesia. *Anesth. Analg.* **115**, 1148-1154  
<https://doi.org/10.1213/ANE.0b013e3182501b04>
- Soboloff J, Rothberg BS, Madesh M, Gill DL (2012): STIM proteins: dynamic calcium signal transducers. *Nat. Rev. Mol. Cell Biol.* **13**, 549-565  
<https://doi.org/10.1038/nrm3414>
- Sobradillo D, Hernandez-Morales M, Ubierna D, Moyer MP, Nunez L, Villalobos C (2014): A reciprocal shift in transient receptor potential channel 1 (TRPC1) and stromal interaction molecule 2 (STIM2) contributes to Ca<sup>2+</sup> remodeling and cancer hallmarks in colorectal carcinoma cells. *J. Biol. Chem.* **289**, 28765-28782  
<https://doi.org/10.1074/jbc.M114.581678>
- Sodero AO, Vriens J, Ghosh D, Stegner D, Brachet A, Pallotto M, Sassoe-Pognetto M, Brouwers JF, Helms JB, Nieswandt B, Voets T, Dotti CG (2012): Cholesterol loss during glutamate-mediated excitotoxicity. *EMBO J.* **31**, 1764-1773  
<https://doi.org/10.1038/emboj.2012.31>
- Sukkar B, Hauser S, Pelzl L, Hosseinzadeh Z, Sahu I, Al-Maghout T, Bhuyan AAM, Zacharopoulou N, Stournaras C, Schols L, Lang F (2018): Inhibition of lithium sensitive Orai1/ STIM1 expression and store operated Ca<sup>2+</sup> entry in chorea-acanthocytosis neurons by NF-kappaB inhibitor wogonin. *Cell Physiol. Biochem.* **51**, 278-289  
<https://doi.org/10.1159/000495229>
- Sun S, Zhang H, Liu J, Popugaeva E, Xu NJ, Feske S, White CL, 3rd, Bezprozvanny I (2014): Reduced synaptic STIM2 expression and impaired store-operated calcium entry cause destabilization of mature spines in mutant presenilin mice. *Neuron* **82**, 79-93  
<https://doi.org/10.1016/j.neuron.2014.02.019>
- Tanwar J, Motiani RK (2018): Role of SOCE architects STIM and Orai proteins in cell death. *Cell Calcium* **69**, 19-27  
<https://doi.org/10.1016/j.ceca.2017.06.002>
- Thorell WE, Leibrock LG, Agrawal SK (2002): Role of RyRs and IP3 receptors after traumatic injury to spinal cord white matter. *J. Neurotrauma* **19**, 335-342  
<https://doi.org/10.1089/089771502753594909>
- Yan J, Zhang B, Hosseinzadeh Z, Lang F (2016a): Down-regulation of store-operated Ca<sup>2+</sup> entry and Na<sup>+</sup> Ca<sup>2+</sup> exchange in MCF-7 breast cancer cells by pharmacological JAK3 inhibition. *Cell Physiol. Biochem.* **38**, 1643-1651  
<https://doi.org/10.1159/000443104>
- Yan J, Zhao W, Guo M, Han X, Feng Z (2016b): CXCL12 regulates the cholinergic locus and CHT1 through Akt signaling pathway. *Cell Physiol. Biochem.* **40**, 982-992  
<https://doi.org/10.1159/000453155>
- Yan J, Fu Z, Zhang L, Li C (2018): Orai1 is involved in leptin-sensitive cell maturation in mouse dendritic cells. *Biochem. Biophys. Res. Commun.* **503**, 1747-1753  
<https://doi.org/10.1016/j.bbrc.2018.07.108>
- Yan J, Zhao W, Gao C, Liu X, Zhao X, Wei T, Gao Z (2019): Leucine-rich repeat kinase 2 regulates mouse dendritic cell migration by ORAI2. *FASEB J.* **33**, 9775-9784: fj201802550R  
<https://doi.org/10.1096/fj.201802550R>

Received: July 1, 2020

Final version accepted: October 7, 2020

Supplementary Material

**Enhanced store-operated calcium entry (SOCE) exacerbates motor neurons apoptosis following spinal cord injury**

Jianye Wang<sup>1,\*</sup>, Wenhui Zhao<sup>2,\*</sup>, Xinjun Wang<sup>1</sup>, Haidong Gao<sup>1</sup>, Rongjun Liu<sup>1</sup>, Jixin Shou<sup>1</sup> and Jing Yan<sup>3</sup>

<sup>1</sup> Neurosurgery Department, The Fifth Affiliated Hospital of Zhengzhou University, Zhengzhou, China

<sup>2</sup> Department of Basic Medicine, Jiangsu College of Nursing, Huai'an, China

<sup>3</sup> Physiology Department, Jining Medical University, Jining, China

Supplementary Figures

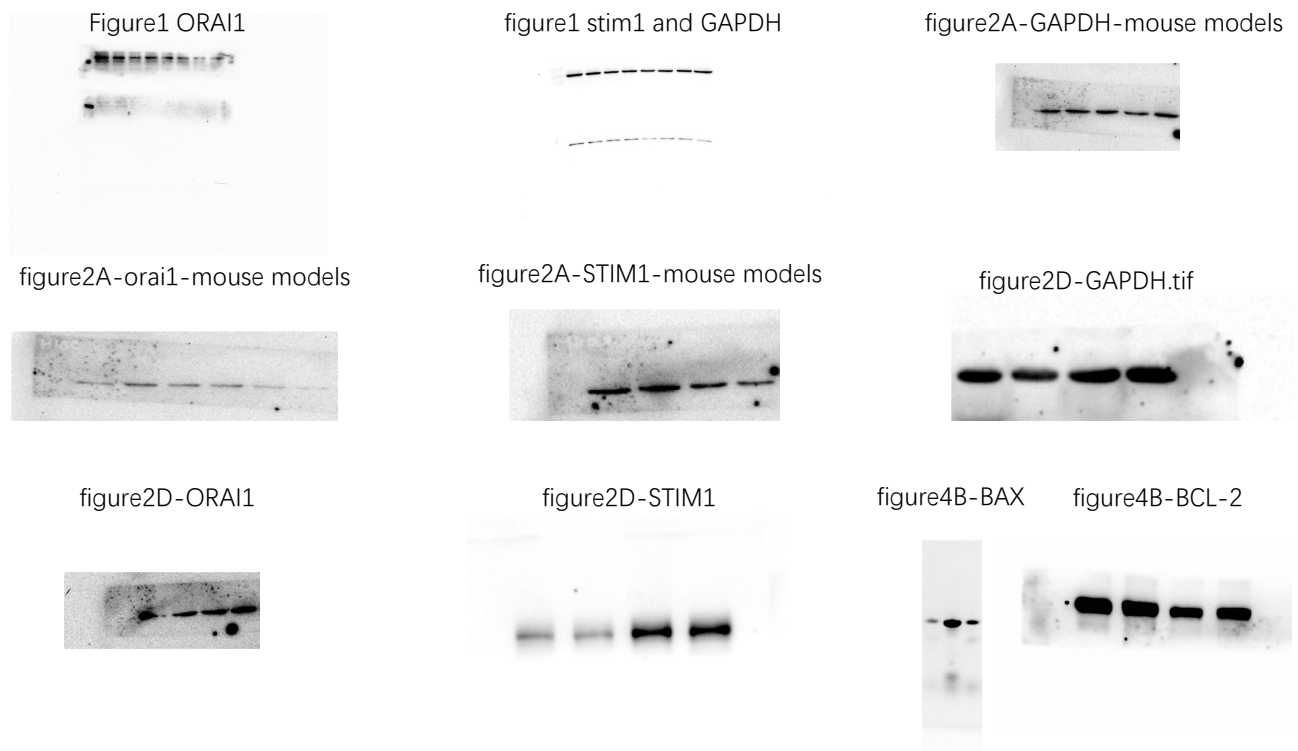


**Figure S1.** Original Western blots of all investigated proteins (blots corresponds to the numbering of figures in the main text).

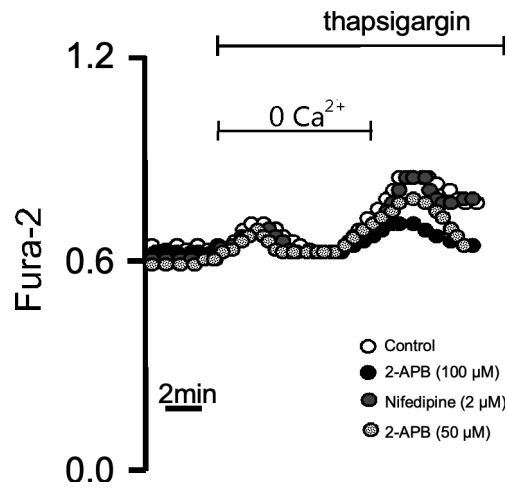


**Figure S2.** 2-APB suppressed SOCE. Representative tracings of fura-2 fluorescence-ratio in fluorescence spectrometry before and following extracellular  $\text{Ca}^{2+}$  removal and addition of thapsigargin ( $1 \mu\text{M}$ ), as well as readdition of extracellular  $\text{Ca}^{2+}$  in VSC4.1 neurons with 2-APB ( $50 \mu\text{M}$ ,  $100 \mu\text{M}$ ) or nifedipine ( $2 \mu\text{M}$ ) ( $n = 30\text{--}40$  cells).